Cellular and Molecular Biology

Journal homepage: www.cellmolbiol.org

Teaching Research on Using Nano Silver Ion Dressing in Clinical Nursing of Surgically Infected Wounds

Haiyan Luo[1], Ni Li[1], Dandan Li[2], Li Xu[1*]

[1]*The Department of Neurosurgery Nursing Unit, The First Affiliated Hospital of Kangda College of Nanjing Medical University/The First People's Hospital of Lianyungang, Lianyungang, 222002, China*

[2]*The Department of Nursing, Kangda College of Nanjing Medical University, Lianyungang, 222002, China*

ARTICLE INFO

Original paper

Article history:
Received: December 01, 2021
Accepted: March 08, 2022
Published: March 31, 2022

Keywords:
Surgical Treatment, Infected Wounds, Clinical Care, Nano Silver Ion Dressing, Antibacterial Properties

ABSTRACT

In real life, there are few occasions where nanomaterials are exposed alone, and more often they coexist with other chemical substances. This article mainly studies the teaching of using nano-silver dressings in clinical nursing of surgically infected wounds. In this paper, the convenience sampling method is used to select 60 patients with chronic wounds as the research objects. A 160μg/mL nano-silver solution prepared with 10% fetal bovine serum DMEM culture medium was dropped on the copper net, and TEM was used for detection. The nanosilver dispersed in different dispersions was divided into 4mL EP tubes and incubated at 4°C, 25°C and 37°C for 0, 3, 12, 24, and 48 hours, and the sample at different time points were detected by a microplate reader. The maximum UV absorption peak was at 300~700nm wavelength. The micro broth dilution method was used to detect the susceptibility of different strains to Ag-PVPNPs and antibiotics. In order to study the relationship between the cytotoxicity of nano silver ion dressings and time, the nano silver ion composite dressings CZ-J1, CZ-J2, CZ-J3, CZ-J4 group samples prepared by the immersion method were selected as test samples, and the test samples were against L02 cells. At different periods, some cloth samples were taken out for anti-adhesion testing. The SPSS19.0 software was used for statistical analysis of the data, and the measurement data were expressed by the mean and standard deviation, and the homogeneity of variance was tested first. The data shows that when combined with 12.5μg/mL Ag-PVP NPs, 2μg/mL gentamicin can completely inhibit the growth of bacteria compared with 50% inhibition rate when acting alone. The results show that nano-silver activated carbon fiber dressing can effectively promote the healing of pressure sore wounds.

DOI: http://dx.doi.org/10.14715/cmb/2022.68.3.30

Introduction

Nanomaterials are different from ordinary materials and have unique physical and chemical properties. Therefore, it is very important to understand the characteristics of the tested nano-silver particles to further explore their toxic effects. Postoperative wound infection causes delayed healing of the incision, which not only adversely affects the surgical effect, but also prolongs the treatment course of the patient and affects the functional recovery of the patient's limbs. On the other hand, the patient may cause more serious complications and even face amputation. Especially after the patient is discharged from the hospital, the effective care of the wound is easily neglected, and even leads to prolonged wound healing, causing secondary harm to the patient's body and mind (1,2).

With the improvement of my country's production and living standards, non-invasive diagnostic technology will have more and more extensive needs. Carrying out research on human trauma diagnosis based on electronic nose technology will help promote the development of my country's olfactory simulation technology, and reduce the international advanced level. The gap, to realize the early diagnosis of human wound infection, has important practical significance. On the one hand, we can obtain the law and mechanism of the combined effect of nano-silver and antibiotics, expand the breadth and depth of the research on the biological effects of nanomaterials, and provide data for the biosafety assessment of related materials; on the other hand, we use the antagonistic system to eliminate nanomaterials and the ecotoxicity of antibiotics provides possible strategies and methods and explores the possibility of using them to fight drug-resistant bacteria by using a combined system with synergistic

*Corresponding author. E-mail: shouzhuo264625195@163.com

effects, providing new ideas for the development of antimicrobial agents, and benefiting mankind (1-3).

Nano silver ion dressings can reduce the risk of wound infection. Fairbrother G believes that in a representative sample of nurses and midwives in Australia, the correlation between self-reported skill levels and behaviors related to evidence-based practice (EBP) should be established. For the EBP competency domain, he explored job satisfaction, mental burnout, and demographic factors to identify models that predict the ability of the population. His survey used an evidence-based practice questionnaire (DEBPQ) and population, job satisfaction and mental burnout index. He used online and paper surveys and distributed them to 405 nurses. He used a stepwise multiple regression procedure to derive a predictive model of EBP skill level and behavior. Although his research is relatively comprehensive, it is not accurate (1). Hong N believes that although robot-assisted surgery has various advantages, it can improve the discontinuous surgical procedure caused by switching between the patient-side manipulator and the endoscopic manipulator, thereby further improving efficiency. Therefore, he proposed a head-mounted host interface (HMI) that can be installed on existing surgical robotic systems and allows continuous surgical procedures using head motion. His proposed system includes HMI, a four-degree-of-freedom endoscope control system, a simple three-dimensional endoscope and a Da Vinci research kit. He performs ten cross-validations to optimize its parameters. He used the result of ten-fold cross-validation and chose an SVM classifier with a Gaussian kernel ($\sigma = 0.85$). He used the SVM classification results to develop an endoscope control algorithm and performed a hook transmission task to check the time-related impact of HMI availability on the system. The algorithm he used can increase the running speed, but it is too complicated (2). Ike S reported that an 80-year-old woman underwent pneumonectomy due to metastasis of pancreatic ductal papillary mucinous carcinoma (IPMC). According to pathological specimens, the primary tumor was diagnosed as aggressive IPMC, pT3N0M0, stage III. A chest CT scan performed 2 years after surgery showed an isolated lung nodule in the lower left lobe. For diagnosis and treatment purposes, he underwent thoracoscopic left lower lobectomy and partial resection of the tongue. Because the phenotype of hematoxylin-eosin staining and mucopolysaccharide secretion in lung lesions is similar to that of primary lesions, it was diagnosed as a metastatic lung tumor by IPMC. Because invasive IPMC usually represents aggressive clinical features, lung metastases are rarely removed. When it is difficult to distinguish primary lung cancer from metastatic cancer, he performed a radical resection of lung cancer. Although his research is innovative, there are some loopholes in the experimental process (3). The purpose of Fu S is to evaluate the impact of laparoscopic surgery courses on laparoscopic surgery skills after simulated training for medical students through the data obtained before and after the laparoscopic simulator training courses for residents standardizing students. the result of. He collected simulator data. After the training level reached the expected goal, he performed simulated cholecystectomy and collected data. Compare the experimental data between the basic group and the special group, and then compare the data between the special group and the experienced group. Although his research methods are relatively safe, they lack the necessary research data (4).

Bacterial infection can lead to the lengthening of the inflammatory phase of the wound, hinder the normal healing process, and make the wound difficult to heal. Clinical often through the injection of antibiotics or antibiotics in the way of drugs to treat a bacterial infection, but with the long-term use of antibiotics, the emergence of super drug-resistant bacteria, the antibacterial effect of antibiotics is declining. Through the physical crosslinking method, the prepared nano silver was introduced into chitosan Luo gum, and the antibacterial gel and antibacterial dressing were prepared, and poloxamer was added to increase the overall water absorption ability of the gel and dressing.

Clinical Nursing of Infected Wounds in Surgical Operation

Surgery

It is similar to surgical vascular ligation or surgical resection of abnormal vessels, instead of surgical resection, to treat or cure the disease with micro trauma technology. After super-selective target organ feeding artery catheterization, embolic agents or embolic substances are injected into the target vessel through the catheter, or the secondary thrombosis is caused by physical action to block the blood flow. However, the

warming effect caused by phototherapy may lead to the local dry microenvironment of the wound, which may lead to delayed wound healing (5-6).

Prandtl liquid dressing is one of the widely used hydrogel dressings in clinical practice. The three-dimensional network containing hydrophilic polymers can provide a moist environment and promote the proliferation of epithelial cells as three-dimensional media. Therefore, carbon light therapy combined with hydrogel dressing can be used as a new physical method for nursing and treating wounds (7). Surgical resection of localized lesions is the main method for the treatment of pulmonary aspergilloma. The principle of operation is to completely remove the lesions while preserving normal lung tissue as much as possible. Pulmonary aspergilloma itself is an inflammatory lesion, and it is easy to cause intrathoracic adhesions. The boundary of the lesion is fuzzy, which brings some difficulties to the integrity of the operation. If the lesion is not completely removed, it is easy to cause more postoperative complications and recurrence. Lobectomy and wedge-shaped resection are the main surgical methods. If the chest wall is involved, partial resection of the chest wall should also be performed. Thoracoscopic or thoracoscopic assisted minimally invasive surgery with improved small incision can achieve small trauma and quick recovery, and all parts of the chest can be observed, which is conducive to intraoperative hemostasis and reduction of blood loss (8-9).

Clinical Care of Infected Wounds

After the initial wound healing, due to the proliferation and contraction of local connective tissue and collagen fibers, scars of varying degrees are formed. The classification recognition rate is defined as:

$$Accuracy = \frac{\sum_{i=1}^{m} x_{ii}}{\sum_{i,j=1}^{m} x_{ij}} \times 100\% \quad [1]$$

Among them, x_{ij} represents the number of test samples of type i that are judged to be type j. The three-point Curtis formula calculates the area under the curve through three equidistant points on the curve, so it can be approximately equal to:

$$I = \int_a^b f(x)dx \approx \frac{b-a}{6}\left[f(x_0) + 4f(x_1) + f(x_2)\right] \quad [2]$$

$$x_k = a + k\frac{b-a}{2}, (k = 0,1,2) \quad [3]$$

For slope, if the slope between each sampling point is calculated, the feature dimension is too large, so this article only calculates the average slope, that is, calculates a response slope every 180 sampling points, so that each sensor gets 10 slope features. The classifier output is expressed as:

$$result = \begin{bmatrix} x_{11} & x_{12} & \cdots & x_{1m} \\ \cdots & \cdots & x_{ij} & \cdots \\ x_{m1} & x_{m2} & \cdots & x_{mm} \end{bmatrix} \quad [4]$$

Among them, x_{ij} represents the number of test samples of type i that are judged to be type j. The mathematical expectation of the loss or difference between the response f(x,w) given by the learning machine and the actual output y of x, that is, the expected risk of the decision function f is:

$$R(w) = E\left[L(y, f(x,w))\right] = \int L(y, f(x,w))dP(x,y) \quad [5]$$

Where f is the decision function. Use known empirical data (training samples) to calculate the risk, and its expression is as follows:

$$R_{emp}(w) = \frac{1}{l}\sum_{i=1}^{l} L(y_i, f(x_i, w)) \quad [6]$$

Let Lagrange function:

$$L(w,b,\alpha) = \frac{1}{2}\langle w \cdot w \rangle - \sum_{i=1}^{l} \alpha_i \left[y_i\left(\langle w \cdot x_i \rangle + b\right) - 1\right] \quad [7]$$

Among them, $\alpha_i \geq 0$ is a non-negative large range multiplier. Skewness S_c and kurtosis K_c are calculated as follows:

$$S_c = \frac{\sum\left(\frac{x_i - \bar{x}}{SD}\right)^3}{N} \quad [8]$$

$$K_c = \frac{\sum\left(\frac{x_i - \bar{x}}{SD}\right)^4}{N} - 3 \quad [9]$$

Among them, x_i, $\bar{x}$ are the i-th measurement value of the gas sensor and the average value of all samples.

The correlation degree of the test results of the two gas sensors can be characterized by covariance or correlation coefficient, and its expression is as follows:

$$Cov(x,y)=\frac{1}{N-1}\sum_{i=1}^{N}(x_i-\bar{x})(y_i-\bar{y}) \quad [10]$$

$$R_{xy}=\frac{\sum_{i=1}^{N}(x_i-\bar{x})(y_i-\bar{y})}{\sqrt{\sum_{i=1}^{N}(x_i-\bar{x})^2\sum_{i=1}^{N}(y_i-\bar{y})^2}} \quad [11]$$

After the hybrid feature construction is completed, the method based on key frames can be used to perform hybrid feature matching and calculate camera motion-related parameters (10). Specifically, the degree of dispersion of each stable feature line is determined by the number of optimized feature points, the number of stable feature lines, and the length of the feature line:

$$N_{temp}=\left[\frac{N_t}{\lambda_p N_p+\lambda_1 N_1}\times\frac{N_1\times L_i}{\sum_{m=1}^{N_1}L_m}\times N_{\max}\right] \quad [12]$$

$$N_i=\begin{cases}2, N_{temp}<2\\ N_{temp}, 2\le N_{temp}\le N_{\max}\\ N_{\max}, N_{temp}>N_{\max}\end{cases} \quad [13]$$

Among them, N_i is the number of points after the ith stable characteristic line is discrete.

When performing image forward matching, suppose the search window of the image feature $I_{k-1}(x_{k-1},y_{k-1})$ of the previous frame is $w_{k-1}(x_{k-1},y_{k-1})$, and the expression for calculating the sum of squares of the pixel difference between the two frames of image feature using $T_{k-1}(u,v)$ as the matching template is as follows.

$$S_k(u,v)=\sum_{u,v}T_{k-1}(u,v)\left[I_k(x_k+u,y_k+v)-I_{k-1}(x_{k-1}+u,y_{k-1}+v)\right]^2 \quad [14]$$

The body's defense response process after trauma includes the inflammatory response initiated by injury and broken tissue cells, which is an aseptic inflammatory process. When a secondary infection occurs, the bacteria also cause an inflammatory response. Although the two types of inflammation are different, it is difficult to distinguish between them in the early stage of clinical diagnosis (11-12). There is a time window from the beginning of pathogenic bacteria multiplying in the wound to the detection of bacteriological and immunological evidence. It is necessary to rely on the experience of the doctor to judge whether it is infected. The two most important methods are to observe the characteristics of the secretion of the wound and the olfactory wound. However, the human olfactory ability is not precise enough, and facing the same wound infection, different doctors often come up with different diagnosis results because of clinical experience or their reasons, that is, subjective (13).

Nano Silver Ion Dressing

When treating wounds, it can effectively absorb wound exudate, kill bacteria in it, maintain a sterile environment, and prevent poisons (such as protein complexes, toxins, bacteria and microorganisms) from penetrating the lymph and blood. The structure of nano silver ions is shown in Figure 1. Because of its adsorption activity, the humidity of the skin and mucous membranes is kept moderate, that is, when the wound has a lot of exudates and affects the growth of the wound, it will absorb the exudate and keep the wound relatively dry and clean (14). When the wound surface loses too much water and is dry and affects the growth of granulation, it can appropriately release the moisturizing elements that are cleaned and filtered by itself, thereby greatly reducing the loss of proteins, hormones, enzymes, vitamins, electrolytes and other substances that are needed by the wound surface. It inhibits the possibility of developing sepsis, significantly promotes the growth of granulation, improves the effect of comprehensive treatment, shortens the treatment period of the disease, and reduces the suffering and mortality of patients (15-16).

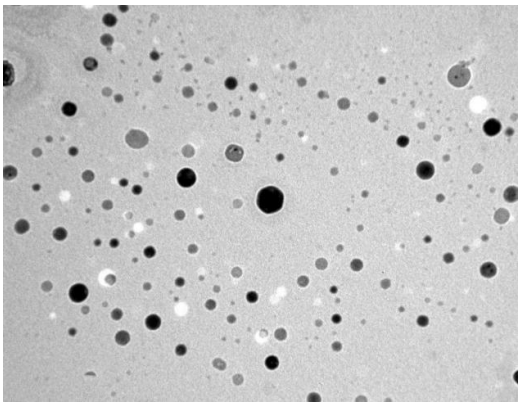

Figure 1. The structure of nano silver ions (this picture is from Baidu http://alturl.com/gebd7)

Materials and methods

Teaching Experiment of Nano Silver Ion Dressing

Subject

Using the convenience sampling method, 60 patients with chronic wounds were selected as the research object. Inclusion criteria: (i) patients with chronic wounds whose duration of the wound was more than 14 days; (ii) patients whose age was more than 18 years old; (iii) patients with normal communication skills; (iv) patients who voluntarily participated in this study; (v) patients who used the concept of wet healing to treat wounds (17).

Preparation of Nano Silver Ion Dressing

A 160μg/mL nano-silver solution prepared with 10% fetal bovine serum DMEM culture medium was dropped on the copper net, and TEM was used for detection. The nanosilver dispersed in different dispersions was divided into 4 mL EP tubes and incubated at 4°C, 25°C and 37°C for 0, 3, 12, 24, and 48 hours, and the sample at different time points were detected by a microplate reader. The maximum UV absorption peak was at a 300~700 nm wavelength. The size of the UV absorption peak can reflect the size of the particles, so investigating the maximum UV absorption peak of the nano-silver solution under different dispersion systems and temperatures can also indirectly reflect the stability of the particles in the solution (18-19).

Cell Culture Fluid Data Collection

In the experiment, the volume of each bacterial culture fluid sample used for data collection is 1 ml, which is placed in a glass petri dish, and the flow value of the mass flow controller (MFC) is set to 100 ml/min. For the time length setting of each stage, the length of baseline collection should ensure that each sensor obtains a stable baseline response, and the length of sample collection should ensure that the gas sensor array produces a sufficient response to the volatiles of the bacterial culture solution to be tested, and the length of system cleaning must ensure that the response of the gas sensor returns to the baseline state to reduce the impact of previous experiments on subsequent experiments (20-21).

Drug Sensitivity Test

The micro broth dilution method was used to detect the susceptibility of different strains to Ag-PVPNPs and antibiotics. In order to study the relationship between the cytotoxicity of nano silver ion dressings and time, the nano silver ion composite dressings CZ-J1, CZ-J2, CZ-J3, CZ-J4 group samples prepared by the immersion method were selected as the test samples, and the test samples were against L02 cells (22).

Anti-Bacterial Adhesion Test

At different periods, part of the cloth samples was taken out for anti-adhesion testing: the cloth samples were rinsed with sterilized PBS solution and then placed in a test tube containing eluent and sonicated for 5 minutes. The sonicated solution was serially diluted to different concentration gradients with a 10-fold dilution method, and 100μL of the bacterial solution was drawn from the test tube of different concentration gradient bacterial solutions with a pipette for coating culture (23).

Surgical Treatment

At the beginning of the operation, first make a longitudinal incision on the right side of the anterior midline, from the upper end to the xiphoid process, and the lower end to 5cm above the navel, and then gradually cut down to the abdominal cavity. Then after determining the spleen injury and the location of the liver and spleen, hold up the spleen by hand, and fill the lower end with warm water gauze to completely expose the spleen pedicle. After ligating and cutting the short gastric artery, carefully separate the splenic pedicle so that the splenic artery and vein can be displayed. Double ligation of the splenic artery with surgical

sutures, and then cut off the splenic artery and vein at the splenic pedicle. After cutting the spleen pedicle, take out the spleen. After the wound model is created, use a sterile cotton swab to stick the pus secreted from the wound and put it into a sterile centrifuge tube (24).

Statistical Processing

Use SPSS19.0 software for statistical analysis of data. The measurement data are expressed by mean and standard deviation. First, the homogeneity of variance test is performed. If the variance is uniform, the t-test is used. If the variance is not uniform, the non-parametric test is used; the count data is used Chi-square test, with $P<0.05$ as the difference is statistically significant.

Results and discussion

Optimization Results of Bacterial Culture Fluid Sample Data

Under different lighting times and distances, the percentage of wound defect area is shown in Figure 2. In Figure 2a, when the light source is 20cm away from the hydrogel, the dehydration effect of the hydrogel is not obvious. When the distance from the light source to the hydrogel decreases from 15cm to 5cm, the dehydration effect of the hydrogel increases significantly. At the same time, the research results show that with the prolongation of the light duration, especially when the light duration is ≥20min, the dehydration effect of the hydrogel tends to increase significantly. When the light duration is set to 5min-15min, the dehydration effect is not obvious. Figure 2b shows that when the light duration is less than 15 minutes, the fibroblasts retain high viability (>85%), and when the light duration is greater than 15 minutes, the cell survival rate is significantly reduced. Moreover, once the light distance is ≤20cm, the survival rate of fibroblasts is significantly reduced (<85%). However, it is worth noting that the silver nanoparticles loaded by the higher concentration of silver nitrate exceed 1%, which greatly exceeds the silver content required for antibacterial. It not only wastes resources but also too high silver content will produce negative effects. The environment causes certain side effects, so we choose 0.2g/L silver nitrate as the experimental concentration.

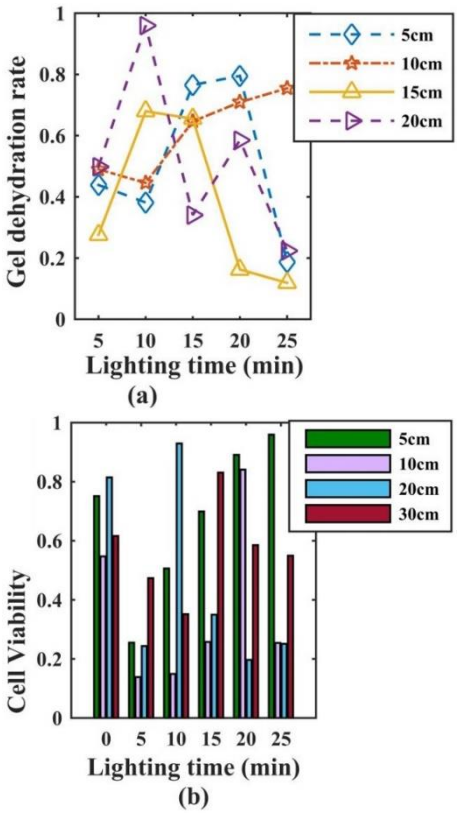

Figure 2. Percentage of wound defect area under different light time and distance

The appearance of the wound at different time points is shown in Figure 3. From the 4th day after the injury, the wound healing effect of the G&C group was significantly better than the other three groups. The new skin tissue in the CPT group can fill the skin defect before 14 days and heal completely before 16 days. In the GEL group, the wound was almost completely healed on the 16th day, but there were still some wounds. In the BLA group, the wound defect was still visible to the naked eye on the 16th day. The trend graph of the wound area is consistent with the external image of the wound.

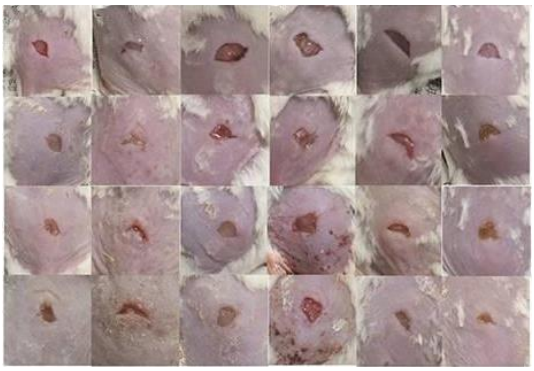

Figure 3. Wound appearance at different time points (this picture is from Baidu http://alturl.com/me3fd)

The parameter statistics of the PVA-Q electrospun fiber membrane are shown in Table 1. With the increase of QAS content, the fiber diameter decreases slightly and the diameter distribution becomes wider. This is because the added QAS has a positive charge, which increases the conductivity of the spinning solution, and the increase of the conductivity will cause a decrease in the fiber diameter. The pore size of the fiber is between 3-5μm and the porosity is between 60-80%. The high porosity gives the PVA-Q fiber membrane good air and water permeability, which meets the requirements of its use as a wound dressing.

Table 1. Parameter statistics of PVA-Q electrospun fiber membrane

Sample	QAS(wt%)	Diameter(μm)	Pore size(μm)	Porosity(%)
PVA	0	0.79±0.15	3.17±0.41	72.8±2.1
PVA-Q5	5	0.78±0.11	4.65±0.35	69.7±1.9
PVA-Q8	8	0.71±0.12	3.45±0.29	70.4±3.8
PVA-Q10	10	0.69±0.10	4.17±0.38	63.0±4.2
PVA-Q12	12	0.68±0.14	2.97±0.42	76.5±1.5
PVA-Q15	15	0.69±0.23	3.84±0.26	68.2±3.0

The results of in vitro cytotoxicity characterization are shown in Figure 4. After co-cultivating the extract of L929 cells and fiber membranes for 0-72h, the absorbance value was measured at 630nm in a microplate reader. The results showed that the absorbance value of the sample group was similar to that of the blank group, indicating that the L929 cell proliferation status was good, and with the incubation time was prolonged, and the number of cells gradually increased. After converting the absorbance value to a relative increase rate, it was found that the relative proliferation rate of the cells cultivated by the PVA-Q cross-linked fiber membrane extract was above 95%, which is 0-level toxicity, and L929 The cell growth morphology showed a shuttle, indicating that the cells grew well. The gel without nano-silver has superior biocompatibility.

The relationship between operation time and surgical site infection is shown in Table 2. The relationship between the duration of operation and surgical site infection, less than 3 hours of operation in 2 cases of infection, the infection rate was 1.76%, more than 3 hours of operation in 3 cases of infection, the infection rate was 2.68%, operation time < 3 hours compared with ≥ 3 hours, operation time < 3 hours was significantly lower than ≥ 3 hours of infection rate, the results showed that the difference was statistically significant ($P < 0.05$). This is mainly because with the increase of the concentration of silver nitrate, the content of silver ions accumulated on the surface of the fiber membrane gradually increases at the same time. After ascorbic acid reduction, the content of nano silver also increases, which makes the color of the fiber membrane surface gradually darker.

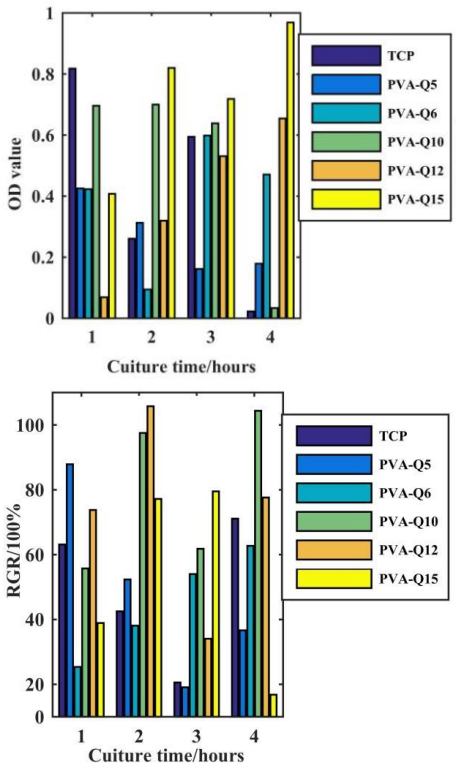

Figure 4. *In vitro* cytotoxicity characterization results

Table 2. The relationship between operation time and surgical site infection

Operation time (h)	Number of operations	Number of infections	Number of uninfected cases	χ^2	p
<3	1135	2	1133	15.984	0.006
≥3	112	3	109		

Comparison of Clinical Indicators

The classification recognition rate results are shown in Figure 5. By selecting the sensor combined with the highest classification recognition rate in the test set, the goal of sensor array optimization is achieved. In optimization method 1, when the first 25 sensors are selected, the classification recognition rate of the test set reaches the maximum and is 88.20%. In optimization method 2, when the first 19 sensors are selected, the selected sensor combination is optimal, and the classification recognition rate reaches the maximum and is 93.08%.

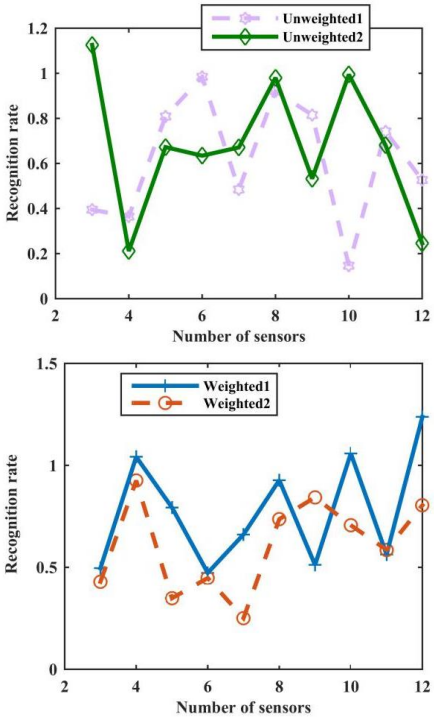

Figure 5. Classification recognition rate results

A549 and HepG2 cells were exposed to different concentrations of silver nanoparticles for 24 and 48 hours, and the results of intracellular silver content detection are shown in Table 3. A549 and HepG2 cells exposed to different concentrations of silver nanoparticles showed a dose-dependent increase in intracellular silver content after 24 and 48 hours, but did not show a time-dependent increase, which showed that at low doses (20μg/mL) the amount of silver uptake by cells in 24h was less than 48h; At high doses (80, 160μg/mL) the amount of silver uptake by cells in 24h is greater than 48h. It shows that the uptake of nano-silver by cells is related to the exposure dose and incubation time. Comparing the silver content of the two cell lines under the same exposure conditions, the results showed that the silver content of HepG2 cells in each dose group was greater than that of A549 cells after 24h exposure; the silver content of HepG2 cells in each dose group was less than A549 cells after 48h exposure.

Table 3. Detection results of intracellular silver content

AgNPs(μg/mL)	A549		HepG2	
	24h	48h	24h	48h
0	ND	ND	ND	ND
20	10.17±1.36	59.85±8.03	22.93±1.01	26.28±4.55
40	55.21±2.80	66.33±21.54	84.29±27.24	48.88±4.62
80	180.36±27.66	155.72±20.45	306.62±20.28	129.67±8.38
160	612.13±44.76	416.57±53.55	739.84±51.66	256.67±3.1

The change curve of the BF structure is shown in Figure 6. The relationship between preoperative antibiotic administration and surgical site infection, antibiotics administered within 0.5 to 1 hour before surgery is considered standard, antibiotics administered more than 1 hour before surgery is considered irregular, and the number of infections in standard medication is 3 For example, the infection rate was 0.24%, and the number of infection cases in the irregular medication was 2 cases, and the infection rate was 15.38%. Compared with the standardized medication and the irregular medication, the infection rate of the standardized medication was significantly lower than that of the irregular medication. The results showed that the difference was statistically significant ($P<0.05$).

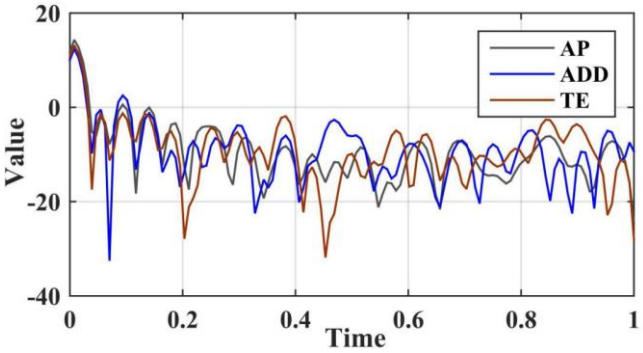

Figure 6. BF structure change curve

The shielding effectiveness test data of fabrics with a different silver content of nano silver ion-plated silver fiber are shown in Table 4 and Figure 7. In the test frequency range, the shielding effectiveness decreases with the increase of the interlacing distance of silver-plated filament at the same frequency. With the increase of frequency, the shielding effectiveness

decreases and the shielding effectiveness becomes worse.

Table 4. Shielding effectiveness test data of fabrics with nano silver ion silver-plated fibers with different silver content

Nano silver ion fiber content	20.0	25.0	30.0	35.0	40.0	45.0	50.0
10	27.0	35.5	38.2	44.2	47.7	53.4	66.5
50	19.0	30.4	37.0	43.2	46.5	53.0	60.4
100	15.6	29.6	36.8	42.5	46.0	52.2	58.5
500	14.3	29.2	36.6	41.5	45.8	51.1	58.3
1000	13.0	28.0	35.1	38.9	45.0	50.1	56.0
2000	12.8	27.6	32.0	37.8	44.8	49.3	54.7
3000	12.5	27.0	29.0	36.4	44.5	48.5	53.8

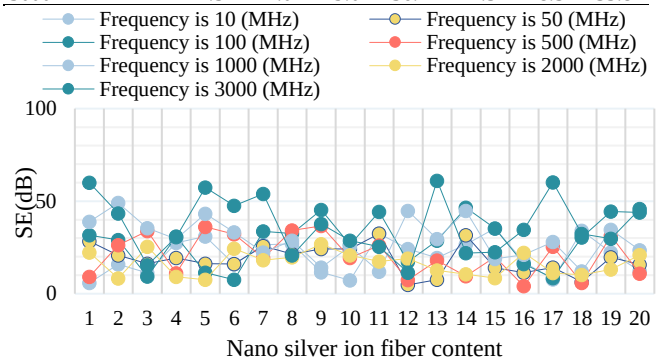

Figure 7. Shielding effectiveness test data of fabrics with nano silver ion silver-plated fibers with different silver content

Influence of the Content of Nano Silver on the Antibacterial Effect

Table 5 shows the comparison of the IOD value and MOD value of each group. After a one-way analysis of variance, the nano-silver activated carbon fiber dressing group was compared with the nano-silver group, activated carbon group, and chlorhexidine petrolatum group. The MOD value and IOD value were higher, and $P<0.05$, there was a difference. It shows that the amount of VEGF released in the nano-silver activated carbon fiber dressing group on the 7th day after pressure sore is more than that of other experimental groups. Compared with the activated carbon group, the nano-silver group had no significant difference with $P>0.01$, indicating that the amount of VEGF released from the wounds of the two groups was relatively consistent. It can be seen from the figure that the PVA-Q10 fiber membrane exhibits antibacterial activity within 3h, and can inhibit the proliferation of Staphylococcus aureus within 6h. When the QAS content is higher than 10%, the number of colonies on the agar plate is further reduced, within 24h the survival rate of Staphylococcus aureus continues to decrease, indicating that PVA-Q fiber membranes with different QAS content have antibacterial effects on Staphylococcus aureus, but PVA-Q5 and PVA-Q8 cannot completely inhibit bacterial growth, and the bacteria remain after 12h. There is a survival rate of more than 30%. When the added QAS content is higher than 10%, the bacterial survival rate is greatly reduced. Among them, PVA-Q12 and PVA-Q15 and Staphylococcus aureus after 3 hours of co-cultivation show obvious antibacterial. The antibacterial rate reached 99.28% and 99.82%, and 99.99% of Staphylococcus aureus could be killed after 6 hours.

Table 5. Comparison of IOD and MOD values of each group

Group	Samples	IOD	MOD
A	10	168927.9±15274.40	0.1374±0.01243
B	10	140946.2±14402.57	0.1147±0.01172
C	10	140873.7±11365.99	0.11464±0.00924
D	10	126378.5±19756.32	0.102851±0.01607
E	10	119970.7±26940.59	0.09763±0.02192

The effect of Ag-PVP NPs and gentamicin alone or in combination on the survival rate of bacteria is shown in Figure 8. As the concentration of Ag-PVP NPs and gentamicin in the combined system increases, the survival rate of bacteria gradually decreases. Therefore, the synergistic antibacterial effect of the two antibacterial drugs is concentration-dependent. When the concentration of Ag-PVP NPs was 12.5μg/mL, the inhibition rates of Escherichia coli ATCC25922 and Staphylococcus aureus ATCC25923 were only 20% and 30%, respectively. However, when gentamicin was present (even at a low concentration of 1μg/mL), Ag-PVP NPs at 12.5μg/mL inhibited the growth of E. coli ATCC25922 and Staphylococcus aureus ATCC25923 by 97% and 80%, respectively. When combined with 12.5μg/mL Ag-PVP NPs, 2μg/mL gentamicin has a 50% antibacterial rate compared to the single action, which can completely inhibit the growth of bacteria.

The moisture retention curve of the sample is shown in Figure 9. The samples prepared by blank CS and soaking method have good moisture retention, and can still retain water for more than 16 hours after exposure to a dry environment. On the first day of the test, the swelling ratio of blank CS and all composite dressings samples was in the range of 20-26; in the subsequent

test time, with the extension of time, the swelling ratio increased slightly. It is confirmed that when the light source is 20cm, the dehydration effect of hydrogel is not obvious. When the light source was reduced from 15cm to 5cm, the dehydration effect of hydrogel increased significantly. At the same time, with the extension of light duration, especially when the light duration is longer than 20min, the trend of dehydration effect of hydrogels increases significantly. However, the dehydration effect was not obvious when the light duration was set at 5-15 min.

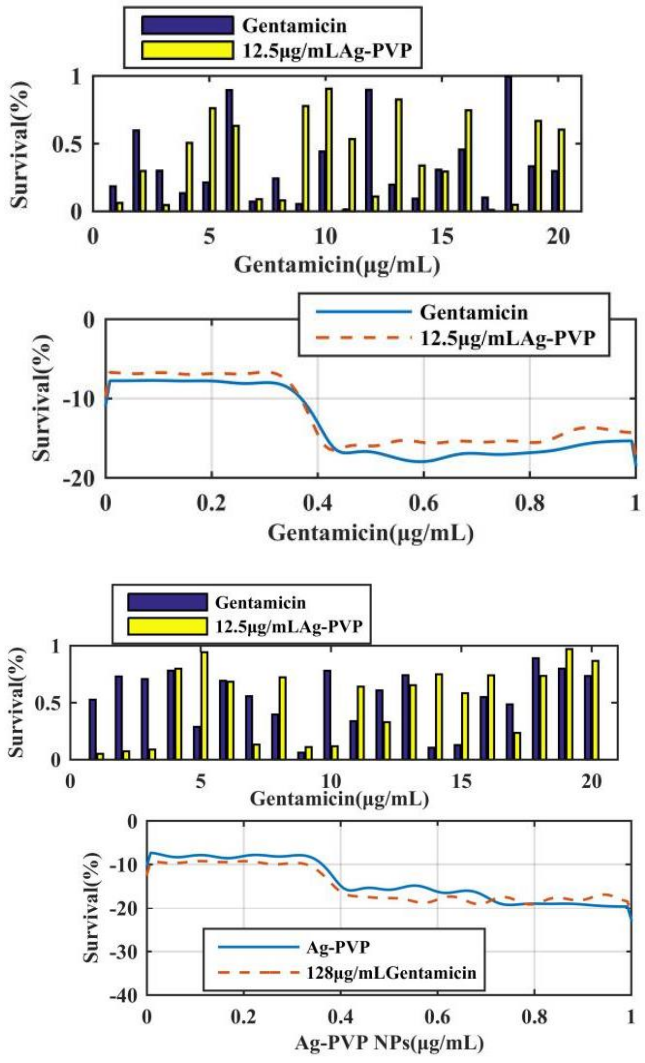

Figure 8. The effect of Ag-PVP NPs and gentamicin alone or in combination on bacterial survival

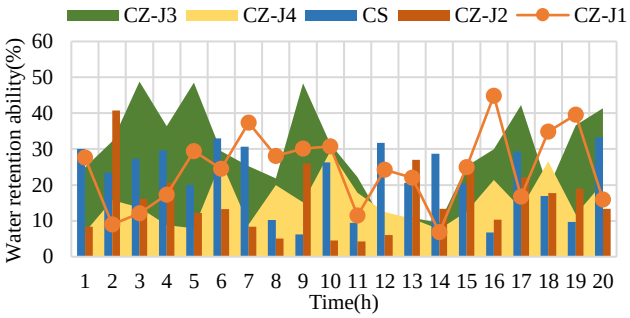

Figure 9. The moisture retention curve of the sample

The results of fibroblast survival showed that when the light duration was less than 15 min, fibroblasts retained high viability, while when the light duration was more than 15 min, the cell survival rate decreased significantly. Moreover, the survival rate of fibroblasts decreased significantly when the light distance was less than 20 cm. Totally, AgNPs in a combination with biocompatible polymers such as Ag-PVP NPs can enhance antibacterial activity suitable for wound dressing application (25-27).

Conclusions

In this paper, a nano-silver dressing was prepared, and its components were characterized and its physical properties were determined. The antibacterial properties of common bacteria, the normal cytotoxicity to the human body and the in vitro procoagulant properties were tested to evaluate its in vitro biological activity. Through SEM observation, it is found that the composite dressing has a loose and porous structure, and zinc oxide and silver-loaded zinc oxide are evenly distributed on the surface and inside of the dressing.

Patients with chronic wounds have a low overall level of knowledge about wound self-care, and health education should pay more attention to older, less educated, and unemployed patients. The pNaMAA grafted cotton fabric loaded with silver nanoparticles can still maintain an anti-bacterial adhesion rate above 99.5% when it is in contact with bacteria for a long time and has good anti-bacterial adhesion and biofilm formation capabilities. The large-scale production and broad application prospects of nano-silver materials have made their antibacterial properties and bio-safety receive extensive attention, but the research on the biological effects of nano-silver in the combined system is very limited.

According to the histopathological score, assess whether the epidermal structure is damaged, whether

the dermis is connected to the epidermis, whether there are blisters, whether the collagen bundles and skin structure are damaged, whether the epidermis is regrown, and whether granulocytes infiltrate. The number of neutrophils in each group must be observed under a 400-fold light microscope. Coating a polyester protective film on the surface of the nano silver ion silver-plated fiber will reduce the antibacterial zone of the silver-plated fiber. The silver-plated fiber produced by the nano-silver ion process has better antibacterial efficacy under the condition of the same silver content. The cost of silver-plated fiber guarantees significant advantages in large-scale industrial production.

Acknowledgments

Not applicable.

Interest conflict

The authors declare that they have no conflict of interest.

References

1. Fairbrother G, Cashin A, Rafferty R, et al. Evidence based clinical nursing practice in a regional Australian healthcare setting: Predictors of skills and behaviours. Collegian 2016; 23(2):191-199.
2. Hong N, Kim M, Lee C, et al. Head-mounted interface for intuitive vision control and continuous surgical operation in a surgical robot system. Med Biol Eng Comput 2019;57(3):601-614.
3. Ike S, Ueda K, Murakami J, et al. A surgical case of solitary pulmonary metastasis after operation for an intraductal papillary mucinous carcinoma. J Jpn Assoc Chest Surg 2017; 31(6):758-762.
4. Fu S, Liu X, Zhou L, et al. Applied Research on Laparoscopic Simulator in the Resident Surgical Laparoscopic Operation Technical Training. India J Surg 2017; 79(4):288-293.
5. Sakellariou, S, Sinclair, et al. Does preoperative breast MRI significantly impact on initial surgical procedure and re-operation rates in patients with screen-detected invasive lobular carcinoma?. Clinical Radiology: R Coll Radiol 2016; 71(6):543-550.
6. Dell'Aquila, Angelo M, Landwehrt J, Scherer M, et al. Strategies for Treatment of Cardiac Ischemic Complication After Heart Surgical Procedures: Is the Reoperation Really the Worst Option?. Ann Thorac Surg 2016; 101(5):2027-2028.
7. Ohya J, Chikuda H, Oichi T, et al. Seasonal Variations in the Risk of Reoperation for Surgical Site Infection Following Elective Spinal Fusion Surgery: A Retrospective Study Using the Japanese Diagnosis Procedure Combination Database. Spine 2017; 42(14):1068-1079.
8. Johnston, Lily, E, et al. Good at One or Good at All? Variability of Coronary and Valve Operation Outcomes Within Centers. Ann Thorac Surg 2018; 105(6):1678-1683.
9. Samuele, Iesari, Quirino, et al. Infected Nonhealing Wound in a Kidney Transplant Recipient: Successful Treatment With Topical Homologous Platelet-Rich Gel. Exp Clin Transplant 2017;15(2):222-225.
10. Terwase, Jerry, Agah, et al. Antibiotic Susceptibility Pattern of Gram-Negative Bacteria Isolated from Infected Wound of Patients in Two Health-Care Centers in Gboko Town. J Clin Case Rep 2018; 8(2):1-5.
11. Reza, Kouhkheil, Mohammadjavad, et al. Impact of Photobiomodulation and Condition Medium on Mast Cell Counts, Degranulation, and Wound Strength in Infected Skin Wound Healing of Diabetic Rats. Photobiomodul Photomed Laser Surg 2019; 37(11):706-714.
12. Liu J, Qian Z, Shi Q, et al. An asymmetric wettable chitosan–silk fibroin composite dressing with fixed silver nanoparticles for infected wound repair: in vitro and in vivo evaluation. RSC Adv 2017; 7(69):43909-43920.
13. Prakoso Y A, Rini C S, Wirjaatmadja R . Efficacy of Aloe vera, Ananas comosus, and Sansevieria masoniana Cream on the Skin Wound Infected with MRSA. Adv Pharmacol Sci 2018; (2):1-7.
14. Fu R H, Weinstein A L, Chang M M, et al. Risk factors of infected sternal wounds versus sterile wound dehiscence. J Surg Res 2016; 200(1):400-407.
15. Agrawal K, Sarda A V, Shrotriya R, et al. Acetic acid dressings: Finding the Holy Grail for infected wound management. Indian J Plast Surg 2017; 50(3):273-280.
16. Boyar, Vita. Efficacy of Dialkylcarbamoylchloride-Coated Dressing in Management of Colonized or Infected Neonatal and Pediatric Wounds. J Wound Ostomy Continence Nurs 2016; 43(5):547-550.
17. Karishma, Kaushik, Snehal, et al. Abandon or Administer? Moving Beyond Oversimplified Approaches and Developing Strategies That Target the Composite-infected Wound Microecosystem. Wounds 2019; 31(1):33-35.

18. Desmond M V, Flavia P, Fiorentini, et al. Treatment of chronic infected post-oncological wounds with a dermal matrix: Two case studies. J Wound Care 2018; 27(9):558-562.
19. Sanda, Smu-Orehovec, Marko, et al. Defect Reconstruction of an Infected Diabetic Foot Using Split- and Full-thickness Skin Grafts With Adjuvant Negative Pressure Wound Therapy: A Case Report and Review of the Literature. Wounds 2018; 30(11):E108-E115.
20. Ishida K, Noborio M, Nishimura T, et al. Negative pressure wound therapy-assisted dermatotraction for the closure of large open wounds in a patient with non-clostridial gas gangreneAcute Med Surg 2016, 3(2):128-131.
21. Jurkovi, Barto, Benurik, et al. Negative pressure therapy with the ULTRAVAC instillation in the therapy of infected laparotomies with fascitis temporary results of aprospective randomized study. Rozhledy v chirurgii : mesicnik Ceskoslovenske chirurgicke spolecnosti, 2019; 98(4):152-158.
22. Zheng T, Huang J, Jiang Y, et al. Sandwich-structure hydrogels implement on-demand release of multiple therapeutic drugs for infected wounds. RSC Advances, 2019, 9(72):42489-42497.
23. Yang C, Goss S G, Alcantara S, et al. Effect of Negative Pressure Wound Therapy With Instillation on Bioburden in Chronically Infected Wounds. Wounds 2017; 23(4):A36-A37.
24. Tsai D M, Tracy L E, Lee C C Y, et al. Full-thickness porcine burns infected with Staphylococcus aureus or Pseudomonas aeruginosa can be effectively treated with topical antibiotics. Wound Repair Regen 2016, 24(2):356-365.
25. Alavi M, Rai M, Martinez F, Kahrizi D, Khan H, Rose Alencar de Menezes I, Douglas Melo Coutinho H, Costa JGM. The efficiency of metal, metal oxide, and metalloid nanoparticles against cancer cells and bacterial pathogens: different mechanisms of action. Cellular, Molecular and Biomedical Reports 2022, 2(1):10-21.
26. Alavi M, Hamblin MR, Martinez F, Kennedy JF, Khan H. Synergistic combinations of metal, metal oxide, or metalloid nanoparticles plus antibiotics against resistant and non-resistant bacteria. Micro Nano Bio Aspects. 2022,1(1):1-9
27. Alavi M, Rai M. Antisense RNA, the modified CRISPR-Cas9, and metal/metal oxide nanoparticles to inactivate pathogenic bacteria. Cellular, Molecular and Biomedical Reports 2021, 1(2):52-59.